Title
Age-related myelin degradation burdens the clearance function of microglia during aging

Journal
Nature Neuroscience, 19(8)

ISSN
1097-6256

Authors
Safaiyan, Shima
Kannaiyan, Nirmal
Snaidero, Nicolas
et al.

Publication Date
2016-08-01

DOI
10.1038/nn.4325

Peer reviewed

Published in final edited form as:
Nat Neurosci. 2016 August 01; 19(8): 995–8. doi:10.1038/nn.4325.

Age-related myelin degradation burdens the clearance function of microglia during aging

Shima Safaiyan[1], **Nirmal Kannaiyan**[2], **Nicolas Snaidero**[1,3], **Simone Brioschi**[4], **Knut Biber**[4,5], **Simon Yona**[6], **Aimee L Edinger**[7], **Steffen Jung**[6], **Moritz J Rossner**[1,2], **Mikael Simons**[1,3,8,9]

[1]Max Planck Institute of Experimental Medicine, Göttingen, Germany [2]Department of Psychiatry, Ludwig-Maximillian University, Munich, Germany [3]Institute of Neuronal Cell Biology, Technical University Munich, Munich, Germany [4]Department of Psychiatry and Psychotherapy, Freiburg, Germany [5]Department of Neuroscience, University of Groningen, University Medical Center Groningen, Groningen, the Netherlands [6]Department of Immunology, Weizmann Institute of Science, Rehovot, Israel [7]Department of Developmental and Cell Biology, University of California, Irvine, Irvine, California, USA [8]German Center for Neurodegenerative Diseases (DZNE), Munich, Germany [9]Munich Cluster of Systems Neurology (SyNergy), Munich, Germany

Abstract

Myelin is synthesized as a multilamellar membrane, but the mechanisms of membrane turnover are unknown. We found that myelin pieces were gradually released from aging myelin sheaths and were subsequently cleared by microglia. Myelin fragmentation increased with age and led to the formation of insoluble, lipofuscin-like lysosomal inclusions in microglia. Thus, age-related myelin fragmentation is substantial, leading to lysosomal storage and contributing to microglial senescence and immune dysfunction in aging.

Myelin is formed by oligodendrocytes as a multilamellar structure that encloses segments of axons in the CNS of vertebrates[1]. Once myelin is laid down, it is unknown to what extent the sheaths require maintenance and remodeling. Myelin membrane components are metabolically relatively stable, with half-lives on the order of several weeks to months[2, 3]. Nevertheless, protein and lipid turnover is, in general, necessary to replace potentially impaired molecules with new functional copies to combat functional decline[4–7]. How do molecules trapped within the numerous layers of tightly compacted membrane enter the

Correspondence to: Mikael Simons.
Correspondence should be addressed to M.S. (msimons@gwdg.de).

Accession codes. GEO: GSE81230.

Note: Any Supplementary Information and Source Data files are available in the online version of the paper.

Author Contributions

S.S. and M.S. conceived the project, designed experiments and wrote the manuscript. S.S., N.K., N.S., and S.B. carried our experiments, S.S., N.K., N.S., S.B., K.B., S.Y., A.L.E., S.J., M.J.R., and M.S. analyzed the data. M.S. supervised the project.

Competing Financial Interests

The authors declare no competing financial interests.

Europe PMC Funders Author Manuscripts

degradative system? We tested the hypothesis that myelin degradation occurs in part via shedding of myelin fragments into the extracellular space.

We analyzed the white matter of aging mice (up to 24 months) by electron microscopy to search for myelin breakdown products. Multilamellar myelin fragments were detected in the aged brain, some of them associated with myelin sheaths and others in the extracellular space or inside of cells (Supplementary Fig. 1). As fixation artifacts frequently affect the appearance of myelin, we used high-pressure freezing to fix tissue and confirmed the progressive accumulation of multilamellar myelin fragments with age (Fig. 1a,b).

We performed immunohistochemistry to determine whether microglia, the brain phagocytes[8–10], were responsible for the uptake of myelin fragments. An increasing number of myelin basic protein (MBP) and proteolipid protein (PLP) immunoreactive puncta colocalized with ionized calcium binding adaptor molecule 1 (Iba1)-positive microglia with age (Fig. 1c and Supplementary Fig. 1) and occasionally with astrocytes (data not shown). Three-dimensional reconstructions demonstrated that immunoreactive puncta were present inside microglia (Fig. 1c). Since our results suggested that microglia clear away the myelin fragments that accumulate in the aging brain, we compared microglia numbers and appearance in young and old animals. Not only had the number of microglia increased in the white matter of old animals, as reported previously[11, 12], but also the number of microglia in contact with myelin (Supplementary Fig. 2). In addition, we observed a marked increase in the size of scavenger receptor class D member 1 (CD68)-positive lysosomes in microglia with age. This increase was more pronounced in the white matter than in the gray matter (Fig. 1d,e). Similar results were obtained by staining with Lamp1, a marker for late endosomes and lysosomes (Supplementary Fig. 2). Since Mac-2 (also called Galectin-3) is known to be involved in myelin phagocytosis[13], we compared Mac-2 immunostaining in young and old mice. We found that the amount of Mac-2 increased in the white matter with age (Supplementary Fig. 2). Fluorescence-activated cell sorting analysis allowed us to exclude macrophage infiltration into the aging brain (Supplementary Fig. 3).

Next we purified microglia from 1-year-old mice to determine the amount of MBP associated with microglia. Western blot analysis of microglial lysates showed that a large fraction of MBP was of high molecular weight, indicating that it forms detergent-insoluble aggregates in microglia (Fig. 1f). To validate these findings, we prepared sarkosyl-insoluble membrane fractions of microglia lysates. High molecular weight species of MBP also existed in the sarkosyl-insoluble membrane fraction (Fig. 1f). When sarkosyl extractions were performed on purified myelin, virtually the entire fraction of MBP was solubilized, demonstrating that only the aggregated state of MBP is sarkosyl-insoluble (Fig. 1f).

One of the most specific biomarkers for the age of postmitotic cells is the accumulation of sarkosyl-insoluble lipofuscin granules in lysosomes[14, 15]. We confirmed the steady increase in number and volume of lipofuscin granules in microglia with age (Supplementary Fig. 4). We found that lipofuscin granules in microglia were larger in the white matter than in the gray matter (Supplementary Fig. 4). When microglia were co-stained with MBP or FluoroMyelin, we observed that myelin fragments were frequently associated with lipofuscin, suggesting that some of the lipofuscin may arise from myelin membrane

remnants (Fig. 1g). To determine whether myelin debris uptake results in lipofuscin generation in microglia, we added purified myelin to organotypic hippocampal slice cultures. Three days after myelin uptake, lipofuscin was already detected in ~15% of the microglia, where it partially colocalized with internalized myelin (Supplementary Fig. 5). The generation of lipofuscin from myelin was confirmed in shiverer mice, in which myelin sheaths form with only a few wraps that are rapidly broken down (Supplementary Fig. 5). These results not only show that microglia actively clear away myelin, but also indicate that this process is associated with the accumulation of undegradable lysosomal aggregates in microglia of the aging brain.

Given that microglia appear to be involved in myelin clearance, we reasoned that blocking lysosomal degradation should lead to the accumulation of myelin fragments in younger mice. Thus, we generated conditional *Rab7* knockout mice using $Cx3cr1^{creER}$ (refs. 16,17) animals to specifically interfere with lysosomal function in microglia ($Rab7^{\Delta MG}$) (Supplementary Fig. 6). Consistent with late endosomal and lysosomal dysfunction, we detected enlarged Lamp1-positive structures in at least 50% of the microglia of $Rab7^{\Delta MG}$ mice (Supplementary Fig. 6).

Notably, $Rab7^{\Delta MG}$ mice developed MBP-immunoreactive puncta in microglial earlier (9 months, versus 18 months of age in control) and with greater frequency than control mice (Fig. 2a). There was a massive accumulation of lipofuscin within microglia in $Rab7^{\Delta MG}$ mice, and, compared to control mice, lipofuscin was more frequently associated with FluoroMyelin-positive myelin fragments (Fig. 2b,c). The lysosomal inclusions were reminiscent of those observed in microglia in the aging brains of wild-type mice. Additional hallmarks of microglial senescence are shortened and fragmented processes, low-grade activation (as determined by increased major histocompatibility complex II (MHC-II) expression) and a decrease in phagocytotic and macropinocytotic function[14]. Microglia in $Rab7^{\Delta MG}$ mice possessed shorter processes, exhibited premature upregulation of MHC-II and showed a reduced capacity to take up stereotactically injected fluorescein isothiocyanate (FITC)-dextran (Fig. 2d and Supplementary Fig. 7). Consistent with a decline in endocytic function in microglia, we detected multilamellar myelin fragments at increased frequency in microglia of $Rab7^{\Delta MG}$ mice (Supplementary Fig. 7). To corroborate the age-associated changes of microglia in $Rab7^{\Delta MG}$ mice, we isolated microglia from wild-type and $Rab7^{\Delta MG}$ animals and performed RNA-seq analysis. We found that 831 genes (~5% of total) were differentially expressed (550 upregulated, 281 downregulated) in microglia from $Rab7^{\Delta MG}$ as compared to microglia from control mice (with enrichments of twofold or greater; $P < 0.05$; Supplementary Table 1). Pathway analysis showed that genes involved in immune function were among the most differentially expressed (Supplementary Fig. 8). As a comparison we performed RNA-seq analysis of aged vs. young microglia[18, 19]. In aged microglia (15 months old), 814 genes were differentially expressed (653 upregulated, 160 downregulated) as compared to microglia from young (10 weeks) mice (Supplementary Table 1). When comparing these two analyses ($Rab7^{\Delta MG}$ versus control and old versus young), we found a prominent overlap (133 genes) between upregulated genes, with an over-representation of pathways related to immune function ($P < 10^{-9}$; Supplementary Fig. 8). Overall, these results suggest that dysfunction of the lysosomal pathway induces a phenotype associated with aging in microglia.

We hypothesized that increasing myelin breakdown in mice could exceed the degradative capacity of microglia earlier in life. Hence, we analyzed whether a single demyelinating event would be sufficient to induce accumulation of aging pigment in microglia. Feeding mice with cuprizone for 4 weeks causes widespread demyelination that is followed by remyelination. We analyzed mice up to 37 weeks after the demyelinating event and quantified lipofuscin volume in microglia in cuprizone-fed and control mice (Fig. 3a). Lipofuscin increased as early as 9 weeks after cuprizone feeding and continued to increase throughout the experiment (Fig. 3b). Myelin fragments were frequently associated with lipofuscin granules even 37 weeks after cuprizone treatment (Fig. 3c). MHC-II was, as expected, strongly upregulated 9 weeks after cuprizone feeding, indicating microglial activation. More interestingly, MHC-II expression returned to control levels at week 15 and 23, but increased again 37 weeks after cuprizone feeding (Fig. 3d). Thus, age-associated immune activation occurs earlier when the brain has undergone one event of widespread demyelination.

Next we analyzed microglia in a mouse model for Pelizaeus-Merzbacher disease with extra copies of the wild-type *Plp1* gene (PMD mice)[20]. These mice develop relatively normal myelin, but long-term stability of myelin is comprised and a large number of the myelin sheaths are gradually broken down and lost[20]. We confirmed the progressive demyelinating phenotype, which accompanied an increased number of microglia and an upregulation of Mac-2 and MHC-II (Supplementary Fig. 9). Myelin fragments were frequently found within microglia (Fig. 3e). Lipofuscin volume in microglia increased more rapidly in the white matter of PMD mice than in that of wild-type mice (Fig. 3f). These changes were accompanied by a decline in macropinocytotic function of microglia as shown by FITC-dextran uptake experiments *in vivo* and amyloid-β peptide uptake assays *ex vivo* (Supplementary Fig. 9).

In summary, we propose that myelin breakdown contributes significantly to the wear and tear on microglia in the aging brain. Why does myelin overload induce lysosomal inclusions in microglia with time? Myelin is not only an abundant membrane, but also a tightly packed, lipid-rich, and therefore poorly digestible one. We propose that the degradative pathway of microglia represents an Achilles' heel of these cells that is sensitive to overloading. It is therefore possible that microglia develop lysosomal inclusions as a consequence of the increasing burden of myelin degradation (and possibly also oligodendrocyte turnover[7]), which may contribute to microglia senescence and immune dysfunction in the normal aged brain.

Methods

Methods and any associated references are available in the online version of the paper.

Online Methods

Generation of mice with microglia-restricted *Rab7* mutation

Mice carrying a conditional *Rab7* allele where the first exon is flanked by *loxP* sites (*Rab7*$^{loxP/loxP}$; ref. 21) were crossed with mice with a tamoxifen inducible Cre-mediated

recombination system (*Cre-ERT2*) driven by a *CX3CR1* promoter to generate mice whose macrophages and microglia lacked the Rab7 protein. In the latter mouse line the *cre-ERT2* along with a *loxP*-flanked neomycin resistance cassette replaces *CX3CR1* exon 2 (ref. 22). To remove the neomycin resistance cassette from the $CX3CR1^{creERT2\text{-}neo}$ locus by Cre-mediated excision, these mice were crossed to $Ella^{cre}$ (E2A Cre, Deleter-Cre) mice (The Jackson Laboratory, B6.FVB-Tg(EIIacre) C5379Lmgd/J, stock number: 003724). In the obtained chimeric mice ($CX3CR1^{+/creERT2\text{-}neo}$; $Ella^{+/cre}$) removal of the neomycin cassette was confirmed with PCR using the primer pair 5′-CACGGGGGAGGCAGAGGGTTT-3′ and 5′-GCGGAGCACGGGCCACATTTC-3′, which results in amplification of a 500-bp fragment indicative of the $CX3CR1^{+/creERT2}$ locus without the neomycin cassette, and a 1,800-bp product specific for the $CX3CR1^{+/creERT2}$ locus with the neomycin cassette. To remove the $Ella^{cre}$ locus from the chimeric mice with the excised neomycin cassette, these mice were mated with C57BL/6J wild-type mice. PCR reactions were done using two set of primers: sense *Ella* promoter (P1): 5′-AGATGACGTAGTTTTCGCGCTT-3′ and antisense Cre (P2): 5′-TCCG GTTATTCAACTTGCAC-3′; and P3: 5′-TATCTTCTATATCTTCAGGCGC-3′ and P4: 5′-GTGAACGAACCTGGTCGAAATCAG-3′. The combination of P1 and P2 amplified a 387-bp product specific for the $Ella^{cre}$ locus, and the mix of P3 and P4 produced a 223-bp fragment for $CX3CR1^{creERT2}$ locus. To obtain double transgenic mice ($CX3CR1^{+/creERT2}$; $Rab7^{loxP/loxP}$) two sets of breedings were arranged with $CX3CR1^{+/creERT2}$ and $Rab7^{loxP/loxP}$ mice. To genotype the offspring of these breeding sets, two distinct PCR reactions using the combination of P3 and P4 and the following primer pair were done: wild-type *Rab7* allele: 5′-CTCACTCACTCCTAAATGG-3′ and *loxP*-flanked *Rab7* allele: 5′-TTAGGCTGTATGTATGTGC-3′. PCR products amplified by the latter primer pair were a 550-bp band specific for wild-type *Rab7* and a 580-bp band representing the *loxP*-flanked *Rab7* allele (i.e., a *loxP*-flanked allele without the neomycin cassette).

Tamoxifen induction of *Rab7* gene deletion

Conditional deletion of *Rab7* in microglia cells of $CX3CR1^{+/creERT2}$; $Rab7^{loxP/loxP}$ mice was induced by tamoxifen injection at 3 weeks of age. Tamoxifen (Sigma T5648) was dissolved in filtersterilized corn oil to make solution of 10 mg/ml. The solution was protected from light and placed on a roller mixer to be dissolved over night at 37 °C. It was administrated via intraperitoneal injection once every 24 h for 5 consecutive days. The injection dose was determined by weight, using approximately 75 mg tamoxifen/kg body weight. For adult mice, a standard dose of 100 μl tamoxifen/ corn oil solution was effective to induce Cre recombinase activity. Control mice of the same genotype received corn oil vehicle only.

Efficiency of $CX3CR1^{creERT2}$ recombinase-mediated deletion in microglia

To test the activity of Cre recombinase in microglia, $CX3CR1^{+/creER}$;$Rab7^{loxP/loxP}$ mice were crossed to reporter mice carrying a *tdTomato* gene located downstream of a *loxP*-flanked STOP cassette. The offspring of this breeding, $CX3CR1^{+/creER}$; $Rab7^{loxP/+}$; $tdTomato^{+}$, were injected with tamoxifen at 3 weeks of age. To confirm deletion of the *Rab7* gene mediated by *CX3CR1*-driven expression of Cre recombinase, 1 and 6 weeks after tamoxifen injection, microglia were isolated and *Rab7* transcripts measured by relative reverse transcriptase quantitative real-time PCR (RT-qPCR) using primers 5′-

GGAATCGGACGTCTCTGTTG-3′ and 5′-AGTCCCCCAGGATGATGAC-3′, designed with NCBI Primer Blast software. The expression of the target gene was measured in relation to internal levels of *Gapdh* and *Rn18s* as reference genes. The quantitative PCR was performed using SYBR Green PCR Master Mix according to the manufacturer's protocols. The relative change in gene expression was analyzed by the ΔCt method, and normalized to the control samples.

Immunohistochemistry

Animals were anesthetized by intraperitoneal injection of 14% chloral hydrate and perfused transcardially with 4% paraformaldehyde (PFA) using a MPII mini peristaltic pump (Harvard Apparatus) (flow rate: 3 ml/min). Brain tissue was postfixed in 4% PFA overnight and cryoprotected in 30% sucrose in 1× PBS until the brain sank (at least 1 d). The tissue was bound to the specimen block using Tissue-Tek O.C.T., frozen on dry ice and cut in coronal direction using cryostat Leica CM 1900. The sections were collected in cryoprotective solution (25% glycerol and 25% ethylene glycol in PBS). Free-floating sections were rinsed with 1× PBS containing 0.2% Tween-20 in a 24-well plate. Permeabilization was performed in 0.5% Triton X-100 with incubation time varying from 10 to 30 min depending on the primary antibody. To block endogenous mouse tissue immunoglobulins, Fab-fragment goat anti-mouse IgG (1:100, Dianova) was added for 1 h at room temperature. The sections were washed briefly and incubated in 100% blocking solution (2.5% FCS, 2.5% BSA, 2.5% fish gelatin in PBS) for 1 h at room temperature. Primary antibodies, diluted in 10% blocking solution, were added and incubated overnight at 4 °C. On the following day, after washing the sections three times with PBS for 10 min, sections were incubated with secondary antibodies, diluted in 10% blocking solution, for 1 h at room temperature. The sections were washed with PBS followed by distilled H_2O and mounted using fluorescence mounting medium (Dako) on Superfrost Plus slides.

3,3-Diaminobenzidine (DAB) immunohistostaining was performed using VECTASTAIN® ABC Kit standard (Vector Laboratories). Free-floating cryosections were transferred to a 24-well plate and washed three times with PBS. Endogenous peroxidase was blocked with 3% H_2O_2, incubated for 20 min at 4 °C, and washed out with PBS. Then 100% blocking solution (as before) was added to the sections and they were incubated for 20 min at room temperature. The sections were incubated overnight at 4 °C with primary antibodies, diluted in 10% blocking solution. Subsequently, the sections were washed with PBS and incubated with biotinylated secondary antibodies for 1 h at room temperature. After washing, AB solution containing 20 μl reagent A (Avidin DH) and 20 μl reagent B (biotinylated horseradish peroxidase H) in PBS was added to the sections and incubated for 30 min at room temperature. Following three washes, staining was developed using a DAB staining kit (Vectastain, Vector Laboratories). The incubation time varied depending on the primary antibody. The DAB reaction was stopped with distilled water; sections were washed with PBS and placed on Superfrost Plus microscope slides for 2–3 d to dry. The sections were rehydrated in decreasing concentrations of ethanol, and finally in water, stained with hematoxylin for 1 min, dehydrated using increasing percentages of alcohol, cleared in xylol (Chemie Vertrieb GmbH) and mounted with Depex.

To reduce lipofuscin autofluorescence in old brain tissues for immunohistochemistry[23], the sections were dipped briefly in distilled water and treated with 10 mM $CuSO_4$ (Fisher Scientific; Pittsburgh, PA) in a buffer containing 50 mM ammonium acetate and 100 μM EDTA, pH 4.5, for 90 min on a shaker. The sections were washed briefly in distilled H_2O and transferred to PBS. Autofluorescence was removed by means of the dye separation tool on a Leica SP5 confocal microscope.

Antibodies

Primary antibodies: Iba1 (Wako, Cat. No., 019-19741), Mac-2 (Biolegend, Cat. No., 125401) MHC-II (Novus Biologicals, Cat. No., NB100-65541), MBP (Covance, Cat. No., SMI-99), PLP (from K.-A. Nave, Max Planck Institute of Experimental Medicine, Göttingen), MAG (myelin-associated glycoprotein, Millipore, Cat. No., MAB1567), Lamp1 (lysosomal-associated membrane protein 1, Santa Cruz Biotechnology, Cat. No., sc-19992) and CD68 (Bio-Rad, Cat. No., MCA1957GA). Secondary antibodies: for DAB staining we used goat anti-rat biotinylated immunoglobulin G (Vector Laboratories, Cat. No. BA-9400) and for fluorescence microscopy we used Alexa Fluor 488-, 647- and 555-conjugated antibodies (Invitrogen, Cat. Nos. A-11034, A-28175, A-21422, A-21443, A27018 and A27039, respectively).

Electron microscopy

For high pressure freezing, mice were killed by cervical dislocation, and freshly extracted optic nerves were cryofixed using a high-pressure freezer (Leica HPM100) and further processed by freeze substitution and EPON-embedding following the tannic acid–OsO_4 protocol as described in Möbius *et al.* [24]. Ultrathin cross-sections 50 (50 nm) of the retinal ends were obtained with an Ultracut S ultramicrotome (Leica) and contrasted as described previously[25].

For conventional fixed preparations the mouse brain was fixed by transcardial perfusion using 4% paraformaldehyde and 2.5% glutaraldehyde in 0.1 M phosphate buffer containing 0.5% NaCl. The brain was extracted and postfixed in the same fixative solution overnight. The tissue was sectioned into 200-μm-thick vibratome sections. Rostral and caudal regions of the corpus callosum were cut and postfixed in a solution of 1% osmium tetroxide in 0.1 M phosphate buffer (pH 7.4) for 30 min at room temperature. Following washing with distilled water the sections were stained with 0.5% uranyl acetate in 70% ethanol for 1 h, dehydrated in a serial dilution of ethanol, and cleared in propylene oxide, embedded in Epon, and incubated at 60 °C for 24 h. The tissues in Epon blocks were then trimmed and reoriented so that ultrathin (60 nm) cross-sections of the midline corpus callosum could be cut using the ultramicrotome. Ultrathin sections were collected on collodion-coated copper grids.

Image processing and analysis

Images were processed and analyzed with Imaris (64× version 7.7.1) and ImageJ 1.41 image processing software. The quantification was performed with investigators blind to the experimental conditions. To estimate the number of Iba1-positive cells, confocal stacks (step size: 0.8 μm) were captured in the *z*-direction from the whole region of interest with 20× or 40× objectives of a Leica TCS SP5 confocal microscope. An area 1 mm^2 in the region of

interest was selected, and the total number of Iba1-positive cell bodies and as well as the number of Iba1-positive cells with internalized components (such as FITC-dextran, MBP or lipofuscin) were counted using the cell counter plugin in ImageJ. In addition, to confirm the quantification performed by ImageJ, cell counting was done automatically using Imaris software. Briefly, a region of interest was segmented and a spots layer was created (radius scale: 8) for each marker (Iba1 and FITC/MBP/LF) in the corresponding channel, and using those spots the cells were counted automatically. The colocalized spots were determined using a distance threshold set to 0.2 μm.

The sizes of lipofuscin accumulations within at least 40 microglia cells were quantified. Individual cells were analyzed using Imaris software as following. An area of 1 mm^2 in cortical white matter and another in the striatum were chosen and confocal *z*-stacks (step size: 0.8 μm) were acquired with a Leica TCS SP5 confocal microscope (40× objective). A three-dimensional image was generated in ImarisSurpass view. The “surface” option in the tool bar was selected, and then a region of interest including lipofuscin compartment within a single cell was segmented in the third channel (far red). The threshold was manually set to cover the whole volume of the compartment in the cell by creating a surface.

To determine myelin and microglia contact area, confocal *z*-stacks (step size: 0.8 μm) were taken in the striatum with the 40× objective of a Leica TCS SP5 confocal microscope. A three-dimensional image from the whole area was created using the Surpass view in Imaris software. To measure the surface area of each microglia cell in contact with myelin, a single cell, including the cell body and all processes in total focus, was segmented. We ensured the entire cell was covered by choosing the “spots” option in the tool bar and adjusting the appropriate threshold. Next, the area labeled with MBP against myelin around the cell of interest was segmented. By activating the “surface” in the tool bar a surface was created over that area. The total number of spots (representing cell process or cell body) and the number of spots close to the surface (representing myelin) were calculated using distance threshold 0.4 μm. Finally, using these numbers the percentage of cell area in contact with myelin was calculated. 230 cells were analyzed.

Imaris software was used to measure the area microglia processes. Forty cells taken from random regions of the brain were analyzed. Confocal *z*-stacks (step size: 0.8 μm) were acquired from different areas in cortical white matter, corpus callosum and striatum using a Leica TCS SP5 confocal microscope with a 40× objective. A three-dimensional image was generated in Imaris Surpass view. Then a microglia cell, including the whole cell body and all its processes in focus, was segmented as a region of interest. Subsequently, to measure the whole area occupied by the single microglia, a surface was created over the whole cell. Additionally, the cell body of each microglia cell was segmented, and its area was quantified by creating a surface. Eventually, the area of the cell body was subtracted from the whole cell area to obtain the area of microglia processes. To visualize inside the cell, the surface was cut using the clipping plane in Imaris software.

Microglia isolation

For optimal dissociation of tissue samples, brain tissue from mice was dissociated using a Neural Tissue Dissociation Kit (Papain) (Miltenyi Biotec). Briefly, the mice were perfused

with cold PBS, the brain was removed and cut into small pieces, and then the tissue was dissociated by enzymatic digestion. Next, the tissue was dissociated mechanically by wide- and narrow-tipped pipettes until no tissue pieces remained. The suspension was pressed through a 40-μm cell strainer and washed twice with Hank's balanced salt solution (HBSS). To remove myelin, the tissue pellet was resuspended in 37% Percoll (Sigma), overlaid on 70% Percoll in DMEM containing 2% FCS (fetal calf serum), and centrifuged at 500*g* for 30 min. The membrane fraction that formed on the top of the 37% Percoll gradient was removed using a vacuum pump. The thin fraction, containing a single-cell suspension, in the interface between 37% and 70% Percoll was then carefully taken out and washed with the medium and MACS rinsing solution (0.5% BSA and 2 mM EDTA in PBS). Microglia were then isolated from the single-cell suspension by MACS technology. The suspension was incubated with CD11b (microglia) MicroBeads (Miltenyi Biotec) at 4 °C for 15 min, after washing with MACS rinsing solution, the pellet was resuspended in 500 μl of the same buffer, applied to a MACS column placed in the magnetic field, and, after being washed three times with 500 μl MACS buffer, CD11b-positive cells (microglia) were flushed out of the column and centrifuged at 400*g* for 8 min at 4 °C. The pellet was resuspended in 1 ml PBS and washed one more time. The final pellet was flash-frozen in liquid nitrogen and stored at −80 °C for future use.

Preparation of sarkosyl-insoluble membrane fractions

The preparation of sarkosyl-insoluble membrane fraction was performed as described previously[26]. Briefly, the pellet containing 1.5×10^6 microglia isolated from 12-month-old mice resuspended in PBS was resuspended again in 300 μl 10% sarkosyl and 1 μl of 10 μg/ml β-mercaptoethanol and incubated at 4 °C for 4 h on a roller. To prepare the sarkosyl-insoluble fraction, the solution was transferred into Beckman 1.5 ml tubes and centrifuged at 130,000*g* for 35 min at 4 °C. The pellet was resuspended in 1 ml cold TBS (50 mM Tris pH 7.6, 150 mM NaCl) and centrifuged again at 130,000*g* for 35 min at 4 °C. The resulting pellet was washed one more time in cold TBS. The supernatant was removed carefully and the final pellet (sarkosylinsoluble fraction, SIF) was flash frozen and stored at −80 °C for further use. To examine the solubility of myelin membrane in sarkosyl, the same experiment was done with 1.5 μg of pure myelin membrane. Western blotting was performed using a polyclonal MBP antibody (Dako, 1:1,000, Cat. No. A0623).

Myelin isolation and purification

The myelin from 8-week-old C57BL/6 mouse brains was isolated by sequential centrifugation on a discontinuous sucrose gradient according to a protocol previously described[27], with some modifications. The ultracentrifugation was done using a SW41 Ti rotor. The brain tissues were homogenized with a Dounce homogenizer in a solution containing 10 mM HEPES, 5 mM EDTA, 0.3 M sucrose, and protease inhibitor. The homogenized tissue was layered on a sucrose gradient composed of 0.32 M and 0.85 M sucrose prepared in 10 mM HEPES, 5 mM EDTA (pH 7.4) and centrifuged at 75,000*g* for 30 min with low deceleration and acceleration. The crude myelin fraction was removed from the interface, suspended in distilled water and centrifuged at 75,000*g* for 15 min. The pellet was subjected to two rounds of hypo-osmotic shock by resuspension in 10 ml ice-cold water, with centrifugation at 12,000*g* for 10 min. For purification of myelin, the pellet obtained

from the last step was dissolved in HEPES/EDTA buffer and placed over the sucrose gradient; all the centrifugation steps and hypo-osmotic shocks were then repeated as before. Eventually, the purified myelin pellet was resuspended in 1 ml HEPES/EDTA buffer and stored at −20 °C.

Organotypic hippocampal slice cultures

Organotypic hippocampal slice cultures (OHSCs) were prepared from P0–P2 C57BL/6N mice according to a slightly modified protocol[28]. OHSCs were kept in a humidified atmosphere at 35 °C and 5% CO_2. The medium was changed every other day.

To deplete microglia, OHSCs were treated with clodronate disodium salt. Clodronate was solved in ultrapure H_2O in a concentration of 1 mg/ml. OHSCs were incubated with 100 μg clodronate per ml standard culture medium for 24 h at 35 °C. Subsequently, OHSCs were rinsed with warm PBS and placed in fresh culture medium. Microglia-depleted OHSCs were kept at least for 7 d *in vitro* before experiment. The medium was changed every other day.

To replenish microglia, microglia were isolated from 8-month-old wild-type and PMD mice by means of density gradient centrifugation using Percoll (Sigma). Mice were perfused with cold 1× PBS, and the cerebrum alone was homogenized in a HBSS containing 0.5% glucose (Sigma) and 15 mM HEPES using a Dounce homogenizer. The tissue was dissociated mechanically by wide-and narrow-tipped pipettes until no tissue pieces remained. The suspension was applied to a 40-μm cell strainer and washed twice with HBSS. Subsequently, the tissue pellet was resuspended in 75% Percoll (Sigma), overlaid on 25% Percoll in PBS, and centrifuged at 800*g* for 30 min. A cloudy layer, containing microglia, in the interface between 25% and 75% Percoll was then carefully collected and cell pellet was obtained by centrifugation at 200*g* for 10 min. The cell number was adjusted to obtain 1,000 cells/μl. Subsequently, 2 μl of cell suspension (2,000 cells) were added on top of each microglia-depleted tissue slice. The replenished OHSCs were maintained for 2 weeks so that the newly added microglia were distributed evenly and ramified[28].

To perform uptake experiments, 5-carboxyfluorescein (5-FAM)-labeled synthetic human amyloid β (Aβ) peptide with amino acids 1−42 was purchased from AnaSpec and prepared according to instructions described previously[29]. Before adding it to OHSCs, Aβ was sonicated for 10 min in an ultrasound water bath and then mixed by vortex for 2 min. The replenished OHSCs were treated twice with Aβ containing solution (2 μl of a 15 μM solution each time) every second day. OHSCs were analyzed 24 h after the last treatment.

Purified myelin pellets were resuspended in sterile PBS and the protein concentration in the myelin was then measured by Bio-Rad Protein Assay, based on the Bradford method. For immunofluorescence analysis, myelin was labeled with PKH26 (Sigma) and then washed in PBS by centrifugation at 15,000*g*. The final pellet was resuspended in the culture medium. Before adding it to the slice culture, the myelin was sonicated for 10 min in an ultrasound water bath.

To perform myelin uptake experiments, 4 μg of purified myelin was added twice onto each slice twice. The first treatment started 3 d after OHSC culture and the second started 1 d

later. OHSCs were fixed with 4% PFA 3 d after the last treatment with myelin. The medium was changed every second day.

In vivo endocytosis assay

Mice were anesthetized intraperitoneally with a solution (0.15 ml/25 g) containing 4% Rompun™ 2% (xylazine) (Bayer DVM for veterinary professionals) and 12.5% ketamine 10% (Medistar) in 0.9% NaCl, placed into stereotaxic apparatus (Kopf Instruments), and injected with 1.5 μg FITC-conjugated dextran (40 kDa; Molecular Probes, Eugene, OR, USA) in sterile PBS via a glass capillary microinjector at the following coordinates relative to bregma: 0.3 mm anterior, 1.2 mm lateral and 1.2 mm below cortical surface. Seven hours after injection the mice were perfused and the brain tissues were prepared and stained as described above.

Cuprizone treatment

Six weeks after tamoxifen injection, *Rab7* conditional knockout mice ($Rab7^{\Delta MG}$) as well as corresponding control mice ($Rab7^{loxP/loxP}$) were treated with 0.2% cuprizone for 4 weeks. The animals were returned to normal diet for another 4 weeks to induce remyelination and continued on the normal diet for 9, 15, 23 or 37 weeks after cuprizone treatment. Age-matched controls received the normal diet without cuprizone throughout the whole experiment.

Flow cytometry

Eight-week-old and 22-month-old mice (7 per group) were anesthetized with ketamine hydrochloride (Ketavet, Pfizer; 100 mg/kg body weight) and xylazine (Rompun, Bayer HealthCare; 20 mg/kg bodyweight) and transcardially perfused with ice-cold PBS. All following steps were carried out on ice and using ice-cold solutions. Isolation of microglia was carried out as previously described[28]. Briefly, perfused brains were carefully removed, placed into a Petri dish and finely shredded with a scalpel. Subsequently, brain tissue were transferred into a tissue masher tube and slowly homogenized. Brain homogenate was eventually flushed with a Pasteur pipette through a 70-μm strainer filter and rinsed with 50 ml of Gibco HBSS 1× medium (Life Technologies). The cellular fraction was collected into a 50 ml Falcon tube and pelleted by centrifugation. Supernatant was discarded and the pellet was resuspended in a 35% Percoll gradient (GE Healthcare). The myelin fraction was removed by centrifugation on a density gradient as follows: 35% Percoll (bottom) and PBS (top). Centrifugation was carried out at 1,000*g* for 30 min at 4 °C without a break. After centrifugation the myelin fraction had settled at the interface between the two gradients, while the cellular fraction was collected in the pellet. The pellet was resuspended in PBS, centrifuged (pellet wash) and eventually transferred into FACS tubes.

Splenocytes were collected by squeezing fragmented spleen tissue through a 70-μm strainer filter and subsequently rinsed with 50 ml of PBS. The cellular fraction was collected into a 50 ml Falcon tube and centrifuged. The pellet was eventually transferred into FACS tubes.

Brain pellets devoid of myelin, as well as spleen pellets, were treated as follows: 15 min incubation with FC-receptor blocker (1:100), followed by 30 min incubation with anti-

Europe PMC Funders Author Manuscripts

mouse CD45-FITC and anti-mouse CD11b-APC (1:200). Between each step pellets were washed in PBS and centrifuged at 1,000*g* for 5 min at 4 °C. All staining products were provided by eBioscience. Immediately before reading, samples were incubated with DAPI (1:1,000) for 1 min. DAPI is poorly permeable through the cell membrane, and therefore its signal was used to identify and select viable cells.

FACS analysis was performed with and eight-color LSR Fortessa from Becton Dickinson (BD Bioscience). Cells were hierarchically gated as follows: (1) FSC/SSC, selection of the microglia population, depending on cell granularity and dimension; (2) FSC-A/FSC-H, selection of single cells; (3) FSC-A/DAPI, selection of viable cells; and (4) final gating on microglia ($CD11b^{+}CD45^{int}$) and brain macrophages ($CD11b^{+}CD45^{hi}$). Cells with CD45-FITC fluorescence intensity higher than 10^4 were arbitrary considered $CD45^{hi}$. In spleen samples the $CD11b^{+}CD45^{hi}$ population was labeled “splenic macrophages”, while the $CD11b^{-}CD45^{hi}$ population was labeled “splenic”.

RNA sequencing

The sorted cells were homogenized in RLT buffer using QIAShredder (Qiagen), total RNA was extracted using micro-RNeasy Kit (Qiagen) and cDNA was synthesized using the Ovation RNA-Seq System V2 (NuGEN). We used 1 μg of cDNA as the input for the Ion Xpress™ Plus Fragment Library Kit (ThermoFisher Scientific) to generate barcoded libraries. Barcoded libraries were quantified using qRT-PCR (KAPA Library Quantification Kit), pooled and clonally amplified on Ion Spheres (Ion One Touch 200 Template Kit v2, ThermoFisher Scientific) and sequenced on an Ion Proton sequencer (ThermoFisher Scientific).

Data analysis

Raw reads were sorted based on barcodes and were subjected to quality analysis using FASTQC. The sequences were subsequently aligned to the genome of *Mus musculus* (GRCm38/Mm10) using the TMAP aligner with default parameters. The reads mapping to unique locations were quantified using RefSeq Gene Annotations (v73) into genes. Differential gene expression analysis and hypergeometric pathway analysis using KEGG gene sets was performed using a commercial platform (Partek). Genes with fold changes greater than 2 and *P*-values less than 0.05 were considered for further hypergeometric pathway enrichment analysis.

Ethics

All experiments were approved and conducted in accordance with animal protection laws approved by the Government of Lower Saxony, Germany. C57BL/6 mice were used for all experiments. The genotypes and ages of the animals are defined in the figure legends. We combined female and male mice for the experiments. They were kept in groups of three in standard plastic cages and maintained in a temperature-controlled environment (21 ± 2 °C) on a 12-h light/dark cycle with food and water available *ad libitum*.

Statistics

Statistical analysis was done using GraphPad Prism (GraphPad Software, Inc.) and SPSS software. No statistical methods were used to predetermine sample sizes, but our sample sizes are similar to those generally employed in the field. Data distribution was assumed to be normal, but this was not formally tested. To compare two groups, a two-tailed Student's *t*-test was applied. One-way ANOVA followed by Bonferroni's *post hoc* test was performed for comparison of more than two groups. When the sample size was small, a non-parametric test such as the Kruskal-Wallis test followed by the Mann-Whitney test was applied. To analyze the interaction of age and genotype, or age and brain region, two-way ANOVA followed by Bonferroni's *post hoc* test was used. A *P*-value of <0.05 was considered significant in all tests. All values are represented as mean ± s.d.

A Supplementary Methods Checklist is available.

Supplementary Material

Refer to Web version on PubMed Central for supplementary material.

Acknowledgments

We thank K.-A. Nave for providing PLP transgenic mice and W. Möbius for electron microscopy support, which was financed by an ERC Advanced Investigator Grant (Axoglia). The work was supported grants from the German Research Foundation (FOR-1756, SFB-TRR43 and SyNergy Excellence Cluster to M.S.; RO 4076/3-1 and RO 4076/5-1 to M.R.; FOR-1336 and BI 668/5-1 to K.B.), an ERC-Consolidator Grant (to M.S.) and the Tschira-Stiftung (to M.S.). N.K. is a recipient of a Marie-Curie fellowship from the INSENS/ FP7-PEOPLE-2013 (607616) framework.

Data availability

The data that support the findings of this study are available from the corresponding author upon request.

References

1. Nave KA, Werner HB. Annu Rev Cell Dev Biol. 2014; 30:503–533. [PubMed: 25288117]
2. Toyama BH, et al. Cell. 2013; 154:971–982. [PubMed: 23993091]
3. Yeung MS, et al. Cell. 2014; 159:766–774. [PubMed: 25417154]
4. Hildebrand C, Remahl S, Persson H, Bjartmar C. Prog Neurobiol. 1993; 40:319–384. [PubMed: 8441812]
5. Peters A. J Neurocytol. 2002; 31:581–593. [PubMed: 14501200]
6. Bartzokis G. Neurobiol Aging. 2004; 25:5–18. [PubMed: 14675724]
7. Young KM, et al. Neuron. 2013; 77:873–885. [PubMed: 23473318]
8. Hanisch UK, Kettenmann H. Nat Neurosci. 2007; 10:1387–1394. [PubMed: 17965659]
9. Aguzzi A, Barres BA, Bennett ML. Science. 2013; 339:156–161. [PubMed: 23307732]
10. Prinz M, Priller J, Sisodia SS, Ransohoff RM. Nat Neurosci. 2011; 14:1227–1235. [PubMed: 21952260]
11. Mouton PR, et al. Brain Res. 2002; 956:30–35. [PubMed: 12426043]
12. Poliani PL, et al. J Clin Invest. 2015; 125:2161–2170. [PubMed: 25893602]
13. Hoyos HC, et al. Neurobiol Dis. 2014; 62:441–455. [PubMed: 24184798]

14. Streit WJ, Xue QS, Tischer J, Bechmann I. Acta Neuropathol Commun. 2014; 2:142. [PubMed: 25257319]
15. Sierra A, Gottfried-Blackmore AC, McEwen BS, Bulloch K. Glia. 2007; 55:412–424. [PubMed: 17203473]
16. Yona S, et al. Immunity. 2013; 38:79–91. [PubMed: 23273845]
17. Goldmann T, et al. Nat Neurosci. 2013; 16:1618–1626. [PubMed: 24077561]
18. Grabert K, et al. Nat Neurosci. 2016; 19:504–516. [PubMed: 26780511]
19. Hickman SE, et al. Nat Neurosci. 2013; 16:1896–1905. [PubMed: 24162652]
20. Readhead C, Schneider A, Griffiths I, Nave KA. Neuron. 1994; 12:583–595. [PubMed: 7512350]
21. Roy SG, Stevens MW, So L, Edinger AL. Autophagy. 2013; 9:1009–1023. [PubMed: 23615463]
22. Jung S, et al. Mol Cell Biol. 2000; 20:4106–4114. [PubMed: 10805752]
23. Schnell SA, Staines WA, Wessendorf MW. J Histochem Cytochem. 1999; 47:719–730. [PubMed: 10330448]
24. Möbius W, et al. Methods Cell Biol. 2010; 96:475–512. [PubMed: 20869535]
25. Snaidero N, et al. Cell. 2014; 156:277–290. [PubMed: 24439382]
26. Nukina N, Ihara Y. J Biochem. 1985; 98:1715–1718. [PubMed: 2419316]
27. Larocca JN, Norton WT. Curr Protoc Cell Biol. 2007; 3:3–25.
28. Masuch A, Shieh CH, van Rooijen N, van Calker D, Biber K. Glia. 2016; 64:76–89. [PubMed: 26295445]
29. Hellwig S, et al. Sci Rep. 2015; 5:14624. [PubMed: 26416689]

Europe PMC Funders Author Manuscripts

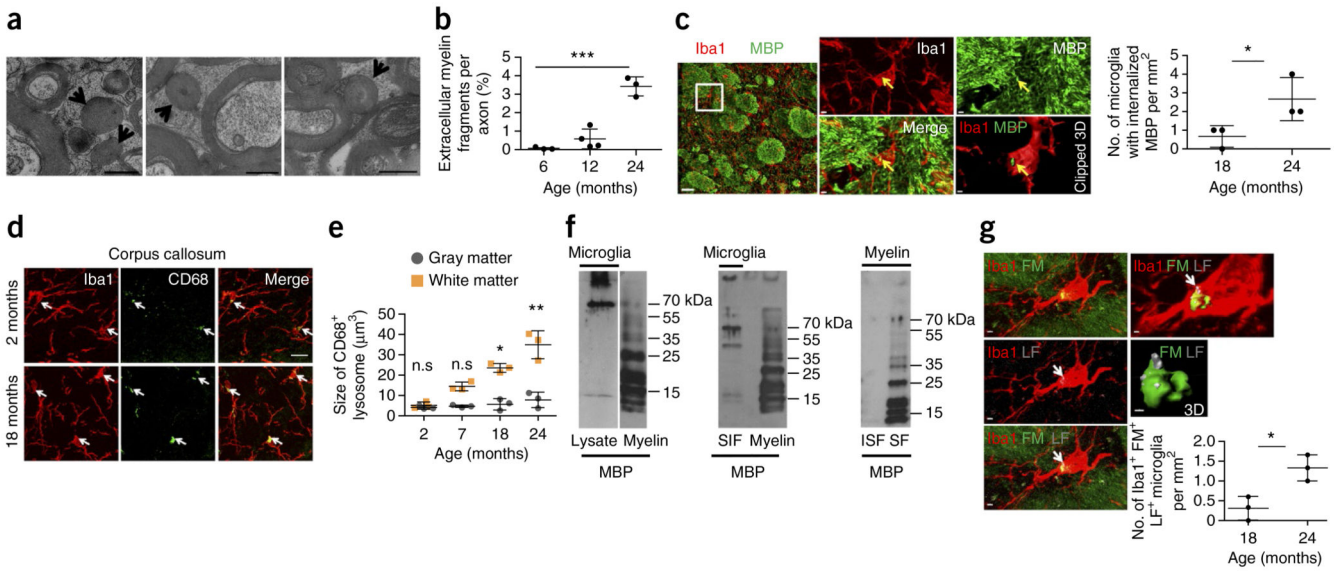

Figure 1. Microglia clear away myelin fragments in the aging brain.

(**a**) High-pressure freezing for electron microscopy was performed on the optic nerve (24-month-old mice shown). Arrows point to myelin fragments; scale bar, 300 nm. (**b**) Quantification of myelin fragments per axon ($n = 3$ mice per group; mean ± s.d.; one-way ANOVA, ***$P < 0.0001$, $F = 50.34$, d.f. = 9; followed by Bonferroni's *post hoc* test, 6 vs. 24 months, ***$P < 0.0001$, $t = 9.253$; 12 vs. 24 months, ***$P = 0.0007$, $t = 8.225$). (**c**) Confocal image shows colocalization of MBP-immunoreactive puncta (green) with Iba1-positive microglia (red) with age. Clipped 3D reconstruction of microglia (see Online Methods) shows MBP (arrows) inside the cell. Scale bars, 30 µm (left); 2 µm (center, top right); 1 µm (clipped 3D). Quantification of number of MBP immunoreactive puncta colocalizing with Iba1-positive microglia in the white matter ($n = 3$ mice per group; mean ± s.d.; *$P = 0.0415$, $t = 2.112$, d.f. = 2; Student's two-tailed t test). (**d**) Visualization of CD68-positive lysosomes (green, marked by white arrows) and microglia (Iba1, red) in wild-type mice. Scale bar, 15 µm. (**e**) Quantification of lysosomal size in microglia of white and gray matter ($n = 3$ mice per group; mean ± s.d.; two-way ANOVA, brain region effect, ***$P = 0.0006$, $F = 20.17$, d.f. = 1; followed by Bonferroni's *post hoc* test, 2 months, $P = 0.7236$, $t = 0.1205$; 7 months, $P = 0.6356$, $t = 1.709$; 18 months, *$P = 0.0321$, $t = 3.139$; 24 months, **$P = 0.0065$, $t = 3.923$). Each dot represents the mean value of 40 cells. (**f**) Left, western blot analysis of purified microglia lysates from 1-year-old mice shows MBP in the high molecular weight region; MBP in myelin is shown as a reference in the right lane. Middle, high-molecular weight species of MBP existed in the sarkosyl-insoluble fraction (SIF) of microglial membranes (1-year-old mice); MBP in myelin is shown as a reference in the right lane. Right, sarkosyl extraction on purified myelin shows that myelin-associated MBP is sarkosyl soluble (sarkosyl-soluble membrane fraction, SF). Full-length blots are presented in Supplementary Figure 10. (**g**) Colocalization of myelin fragments (FluoroMyelin, FM, green) with lipofuscin (LF, gray, marked with white arrows) within microglia (red) in a 24-month-old mouse. Scale bars, 2 µm. Quantification shows number of puncta positive for FluoroMyelin (FM) and lipofuscin colocalizing with Iba1-positive microglia in the white matter ($n = 3$ mice per group, mean ± s.d.; *$P = 0.0356$, $t = 2.513$, d.f. = 3; Student's two-tailed t test). In

Europe PMC Funders Author Manuscripts

b, **c** and **g** each dot represents the mean value of 3 brain slices per mouse. All images are representative of three independent experiments and western blots of five.

Europe PMC Funders Author Manuscripts

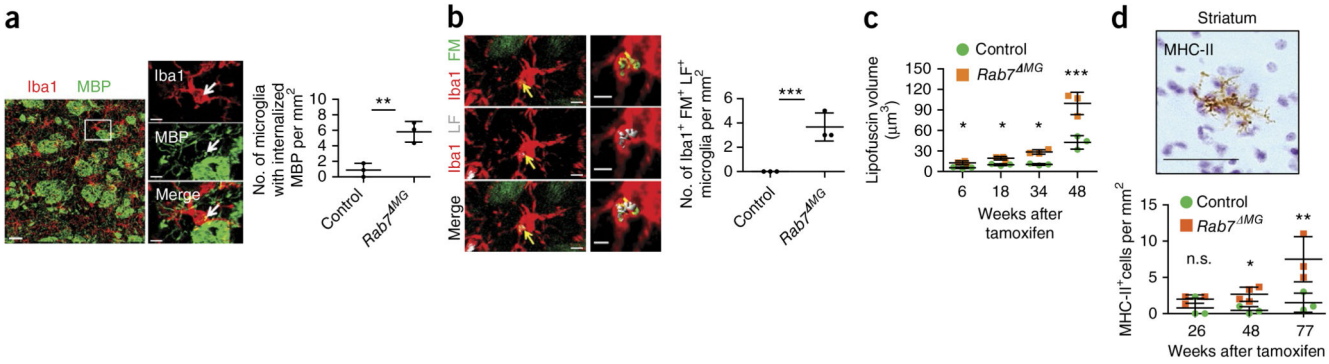

Figure 2. Blocking transport within the lysosomal pathway of microglia results in intracellular myelin storage and age-associated immune activation.

(**a**) Confocal image shows colocalization (white arrows) of MBP (green) with Iba1-positive microglia (red). Scale bars, 30 μm (left); 2 μm (right). Quantification of MBP-immunoreactive puncta in microglia of the white matter in 9-month-old control and *Rab7* $^{\Delta MG}$ mice ($n = 3$ mice per group; mean ± s.d.; $^{**}P = 0.0058$, $t = 5.376$, d.f. = 4; Student's two-tailed t test). (**b**) Colocalization of myelin fragments (FluoroMyelin (FM), green) with lipofuscin (LF, gray) within microglia in 12-month-old mice ($n = 3$ mice per group; mean ± s.d.; $^{***}P < 0.0001$, $t = 21.265$; d.f. = 4; Student's two-tailed t test). Scale bars, 2 μm. (**c**) Quantification of lipofuscin volume in μm^3 in *Rab7* $^{\Delta MG}$ mice as compared to controls ($n =$ 3 mice per group, mean ± s.d.; two-way ANOVA; genotype effect, $^{**}P = 0.0033$, $F = 17.09$; followed by Bonferroni's *post hoc* test; $^{*}P < 0.05$, $^{***}P = 0.0006$, $t = 7.145$). Each dot represents the mean value of 40 cells. (**d**) Visualization and quantification of MHC-II-positive microglia in *Rab7* $^{\Delta MG}$ mice and controls ($n = 3$ mice per group; mean ± s.d.; two-way ANOVA; genotype effect, $^{***}P = 0.0007$, $F = 19.70$; followed by Bonferroni's *post hoc* test; $^{*}P = 0.0412$, $t = 2.893$, $^{**}P = 0.0081$, $t = 4.782$). n.s., nonsignificant ($P = 0.3221$). Scale bar, 50 μm. In **b** and **d** each dot represents the mean value of 3 brain slices per mouse. All images are representative of three independent experiments.

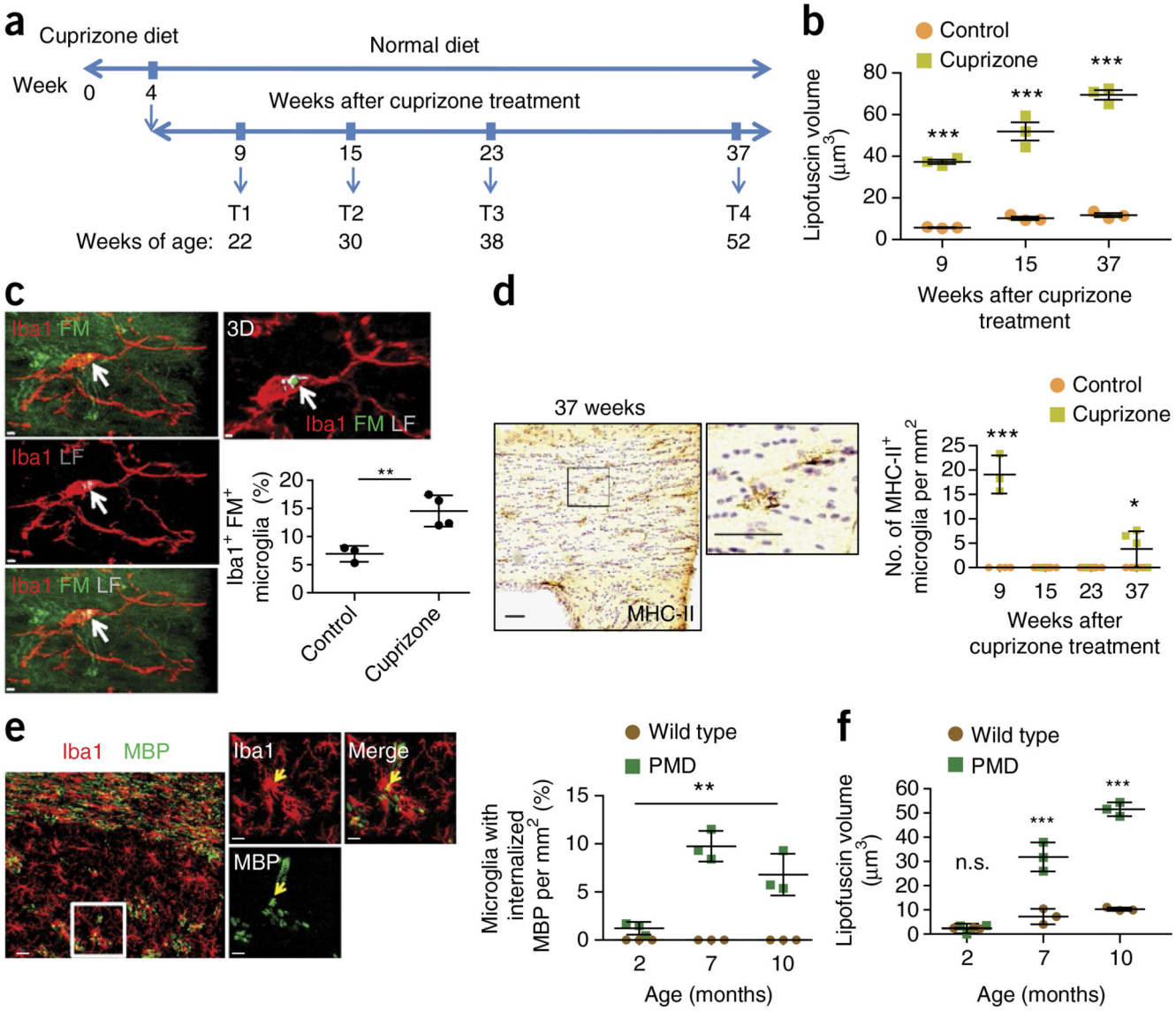

Figure 3. Demyelination leads to lipofuscin formation in microglia with time.

(**a**) Demyelination was induced by feeding mice cuprizone and their recovery was examined according to the timeline. (**b**) Quantification of lipofuscin volume in microglia 9, 15 and 37 weeks after cuprizone treatment ($n = 3$ mice per group; mean ± s.d., two-way ANOVA; cuprizone treatment effect, ***$P < 0.0001$, $F = 389.2$; followed by Bonferroni's *post hoc* test, ***$P < 0.001$). Each dot represents the mean value of 40 cells. (**c**) Colocalization of myelin fragments (FluoroMyelin, green) with lipofuscin (gray) within microglia 37 weeks after cuprizone treatment (8-month-old mice; $n = 3$–4 mice per group; mean ± s.d.; **$P = 0.0078$, $t = 4.289$, d.f. = 5; Student's two-tailed t test). Scale bars, 2 µm. (**d**) Quantification of MHC-II positive microglia in cuprizone-fed mice (9, 15, 23 and 37 weeks after cuprizone treatment as compared to aged-matched untreated mice; $n = 5$ mice per group; mean ± s.d.; two-way ANOVA; cuprizone treatment effect, ***$P < 0.0001$, $F = 26.93$; followed by Bonferroni's *post hoc* test; ***$P = 0.0007$, $t = 8.092$; *$P = 0.0425$, $t = 1.326$). Each dot

Europe PMC Funders Author Manuscripts

represents the mean value of 6 brain slices per mouse. Scale bar, 50 μm. (**e**) Confocal images and quantification of number of MBP-immunoreactive puncta (green) colocalizing with Iba1-positive microglia (red) in 10-month-old wild-type and PMD mice ($n = 3$ mice per group; mean ± s.d.; one-way ANOVA; $^{**}P = 0.0017$, $F = 21.93$, d.f. = 8; followed by Bonferroni's *post hoc* test; 2 vs. 7 months, $^{**}P = 0.0029$, $t = 6.521$; 2 vs. 10 months, $^{*}P = 0.0352$, $t = 4.263$) Scale bars, 30 μm (left); 5 μm (right). Each dot represents the mean value of 3 brain slices of one mouse. (**f**) Quantification of lipofuscin (LF) volume in microglia of 2-, 7- and 10-month-old PMD and wild-type mice ($n = 3$ mice per group; mean ± s.d.; two-way ANOVA; genotype effect, $^{***}P < 0.0001$, $F = 221.6$; followed by Bonferroni's *post hoc* test; 2 months, $P = 0.9232$, $t = 0.0465$; 7 months, $^{***}P = 0.0002$, $t = 9.653$; 10 months, $^{***}P < 0.0001$, $t = 16.18$). Each dot represents the mean value of 40 cells. All images are representative of three independent experiments. n.s., nonsignificant ($P = 0.9232$).

Europe PMC Funders Author Manuscripts